Probabilistic Characterization of 3-D Spatial Variability of Soils: Methodology and Strategy

Te Xiao
Ph.D., State Key Laboratory of Water Resources and Hydropower Engineering Science, Key Laboratory of Rock Mechanics in Hydraulic Structural Engineering (Ministry of Education), Wuhan Univ., Wuhan, China.

Dian-Qing Li
Professor, State Key Laboratory of Water Resources and Hydropower Engineering Science, Institute of Engineering Risk and Disaster Prevention, Wuhan Univ., Wuhan, China.

Zi-Jun Cao
Associate Professor, State Key Laboratory of Water Resources and Hydropower Engineering Science, Institute of Engineering Risk and Disaster Prevention, Wuhan Univ., Wuhan, China.

Li-Min Zhang
Chair Professor, Dept. of Civil and Environmental Engineering, The Hong Kong Univ. of Science and Technology, Hong Kong, China.

ABSTRACT: The 3-D spatial variability of soils has significant impacts on the failure mechanism and reliability of geotechnical structures and deserves a quantitative characterization through site investigation. This study develops a probabilistic approach for characterizing the 3-D spatial variability of soils within the framework of maximum likelihood estimation, whose computational problem is addressed through a matrix decomposition technique. The sampling strategy to minimize the statistical uncertainty is explored systematically based on virtual site analysis. The empirical distance criterion and density criterion are proposed to control the statistical uncertainty to a practically acceptable low level.

1. INTRODUCTION

Subject to various natural processes, soil properties vary in 3-D space and preserve strong anisotropy in vertical and horizontal directions. The 3-D spatial variability of soils has significant impacts on the failure mechanism and reliability of geotechnical structures (Fenton and Griffiths, 2005; Xiao et al., 2016), which cannot be fully captured by the conventional 1-D/2-D spatial variability modeling (Li et al., 2016a; Xiao et al., 2017; Papaioannou and Straub, 2017). In spite of the importance on the quantification of 3-D spatial variability, works on direct characterization make slow progress (Liu and Leung, 2018), due to the scarcity of geotechnical data and a satisfactory characterization method. Most previous studies thus simplify the 3-D characterization as two individual parts, including a vertical spatial variability characterization along the depth of borehole/sounding (Fenton, 1999; Wang et al., 2010) and a horizontal spatial variability characterization in a transverse plane (DeGroot and Baecher, 1993; Ching et al., 2018). Such a treatment cannot make full use of the information contained in the limited geotechnical data.

Among the 3-D spatial variability, the characterization of horizontal spatial variability is relatively more difficult and less investigated than the vertical part, because of the scarcity of test soundings for a majority of projects. Researches should pay more attentions to the horizontal spatial variability characterization, since it plays an essential role in site mapping that extends site-

specific knowledge from limited soundings to the whole site. Considering the high cost of site investigation, it is necessary to design a proper sampling strategy (or testing strategy) to optimize the amount and location of soundings. This idea is not new, and previous probabilistic studies mainly focus on minimizing the mapping uncertainty (Li et al., 2016b) or maximizing the value of information (Yoshida et al., 2018). Both of them highly rely on the results of spatial variability characterization. In the presence of limited geotechnical data, the characterization is usually associated with large statistical uncertainty and, in turn, makes itself and the sampling strategy less robust. Rare studies investigate the sampling strategy from a perspective of minimizing the statistical uncertainty in spatial variability characterization, where this paper would make an effort. The uncertainties involved in the model selection (Cao and Wang, 2014; Ching and Phoon, 2017), such as selection of probabilistic distribution, trend function and correlation function, will not be considered in this study.

This study develops a probabilistic approach for characterizing the 3-D spatial variability of soils within the framework of maximum likelihood estimation (MLE). The vertical and horizontal spatial variabilities are simultaneously characterized based on multiple cone penetration tests (CPTs). A matrix decomposition technique is proposed to bypass the computational problem that hinders the practical application of MLE for high-dimensional and spatially correlated data. With the help of proposed approach, the sampling strategy to minimize the statistical uncertainty is explored and two empirical design criteria are proposed based on virtual site analysis.

2. CHARACTERIZATION OF 3-D SPATIAL VARIABILITY

2.1. Maximum Likelihood Estimation

The 3-D spatial variability of soils is commonly described by random field theory (Vanmarcke, 2010). In the context of MLE, the log-likelihood of n observations, $\boldsymbol{X}$ (e.g., normalized cone tip resistance Q_{tn} of CPT) can be written as (DeGroot and Baecher, 1993; Fenton, 1999),

$$\ln L = -\frac{n}{2}\ln(2\pi) - \frac{n}{2}\ln\sigma^2 - \frac{1}{2}\ln|\boldsymbol{R}| - \frac{1}{2\sigma^2}(\boldsymbol{X}-\boldsymbol{F}\boldsymbol{\beta})^{\mathrm{T}}\boldsymbol{R}^{-1}(\boldsymbol{X}-\boldsymbol{F}\boldsymbol{\beta}) \quad (1)$$

where $\boldsymbol{F}$ and $\boldsymbol{\beta}$ = trend function matrix and coefficient vector, respectively; σ = standard deviation; and $\boldsymbol{R} = [\rho] = n \times n$ spatial correlation matrix, in which the correlation coefficient ρ is described by a prescribed correlation function. For example, a 3-D single exponential correlation function is defined as,

$$\rho = \exp\left(-2\sqrt{\tau_x^2+\tau_y^2}\,/\,\delta_h - 2\tau_z/\delta_v\right) \quad (2)$$

where τ_x, τ_y, and τ_z = relative distance of two locations in x- (horizontal), y- (horizontal) and z- (vertical) directions; and δ_h and δ_v = horizontal and vertical scales of fluctuation, respectively.

By maximizing the log-likelihood function, estimates of the four random field parameters ($\boldsymbol{\beta}$, σ, δ_v, δ_h) can be determined. Among them, estimates of $\boldsymbol{\beta}$ and σ can be derived analytically as functions of $\boldsymbol{R}$, which reduces the number of optimized parameters to only two, namely δ_v and δ_h. Note that repeated calculation of $\ln|\boldsymbol{R}|$ and $\boldsymbol{R}^{-1}$ is needed during the optimization. This is not trivial for high-dimensional CPT data. For example, forty CPTs at a penetration interval of 20 mm and a depth of 20 m contain n = 40×20/0.02 = 40,000 data records. Consequently, the matrix size of $\boldsymbol{R}$ is as large as 40,000×40,000 and extremely high computational effort should be paid for evaluating $\ln|\boldsymbol{R}|$ and $\boldsymbol{R}^{-1}$.

Once the maximum likelihood estimates are found, the associated statistical uncertainty can be represented by covariance or coefficient of variation (COV). By definition, the covariance equals, approximately and asymptotically, the inverse of observed information matrix evaluated at the maximum likelihood estimates, and the COV takes the ratio of the corresponding standard deviation to the maximum likelihood estimates.

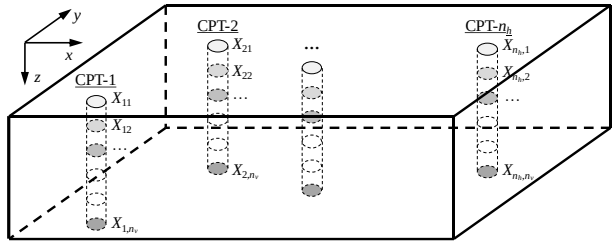

(a) Spatial distribution of CPT data

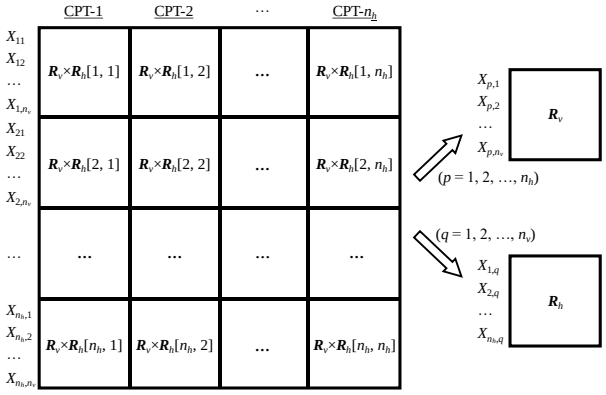

(b) Global correlation matrix

Figure 1: Spatial distribution and correlation of CPT data.

2.2. Correlation Matrix Decomposition

To bypass the aforementioned computational problem of MLE, the CPT data records are deliberately arranged one sounding after another, as shown in Figure 1(a). By this means, the global correlation matrix $\boldsymbol{R}$ is a block matrix as shown in Figure 1(b), and it can be decomposed as $\boldsymbol{R} = \boldsymbol{R}_h \otimes \boldsymbol{R}_v$, where $\otimes$ = Kronecker product; $\boldsymbol{R}_v$ = vertical correlation matrix for data within a sounding; and $\boldsymbol{R}_h$ = horizontal correlation matrix for data at the same depth. As a result, $|\boldsymbol{R}|$ and $\boldsymbol{R}^{-1}$ can be written as,

$$\ln|\boldsymbol{R}| = n_v \ln|\boldsymbol{R}_h| + n_h \ln|\boldsymbol{R}_v| \tag{3}$$

$$\boldsymbol{R}^{-1} = \boldsymbol{R}_h^{-1} \otimes \boldsymbol{R}_v^{-1} \tag{4}$$

where n_v = number of data within a sounding; n_h = number of soundings; and $n_v \times n_h = n$.

Calculations for determinants and inverses of $\boldsymbol{R}_v$ and $\boldsymbol{R}_h$ are much easier than those of $\boldsymbol{R}$. To save computational memory and further improve computational efficiency, avoiding the assembly of $\boldsymbol{R}^{-1}$ is necessary, and it can be achieved with the aid of Kronecker product (Xiao et al., 2018).

Table 1: Scenarios of virtual site analysis.

	δ_v (m)	δ_h (m)	A (m^2)	D (m)	n_h
Value	*0.5*	*10*	*50×50*	*5*	*4*
	1	*20*	*100×100*	*10*	*8*
	1.5	*30*	*150×150*	*15*	*12*
	2	*40*	*200×200*	*20*	*16*

Specifically, the $\boldsymbol{R}^{-1}$ related matrix multiplication $\boldsymbol{A}^{\mathrm{T}}\boldsymbol{R}^{-1}\boldsymbol{B}$ reads as

$$\boldsymbol{A}^{\mathrm{T}}\boldsymbol{R}^{-1}\boldsymbol{B} = \mathrm{tr}\left[\underline{\boldsymbol{A}}^{\mathrm{T}}\boldsymbol{R}_v^{-1}\underline{\boldsymbol{B}}\left(\boldsymbol{R}_h^{-1}\right)^{\mathrm{T}}\right] \tag{5}$$

where $\boldsymbol{A}$ and $\boldsymbol{B}$ = n×1 vectors; and $\underline{\boldsymbol{A}}$ and $\underline{\boldsymbol{B}}$ = $n_v \times n_h$ matrices reshaped from $\boldsymbol{A}$ and $\boldsymbol{B}$, respectively. The matrix decomposition technique decomposes the large global correlation matrix into smaller vertical and horizontal correlation matrices. Considering the nature of CPT that $n_v >> n_h$, it makes the computational effort for 3-D spatial variability characterization almost comparable with that for 1-D vertical spatial variability characterization, and facilitates the practical application of MLE in 3-D spatial variability characterization.

3. SAMPLING STRATEGY

3.1. Virtual Site Analysis

To make a proper sampling strategy, the impact of sampling plan on the statistical uncertainty in 3-D spatial variability characterization is explored systematically through virtual site analysis.

Several virtual sites of CPT parameter Q_{tn} are first simulated using the 3-D random field generation approach (Xiao et al., 2018). For simplicity, this study only considers: (1) a square sampling area A; (2) a CPT penetration interval of 50 mm; and (3) a Gaussian random field with a mean μ = 100 (i.e., $\boldsymbol{F}$ = **1** and $\boldsymbol{\beta} = \mu$), a standard deviation σ = 40, and a 3-D single exponential correlation (i.e., Eq. (2)). Four δ_v values and four δ_h values, as shown in Table 1, are assumed to represent different degrees of the 3-D spatial variability. Besides, different sampling schemes are adopted, with four sampling areas A, four sampling depths D, and four sounding numbers

Table 2: Spatial variability characterization results.

Parameter		μ	σ	δ_v	δ_h
True value		100	40	1	20
Example I	MLE	103.13	41.15	1.12	19.85
	COV	0.08	0.08	0.17	0.12
Example II	MLE	98.45	35.23	0.82	0
	COV	0.05	0.07	0.15	Inf

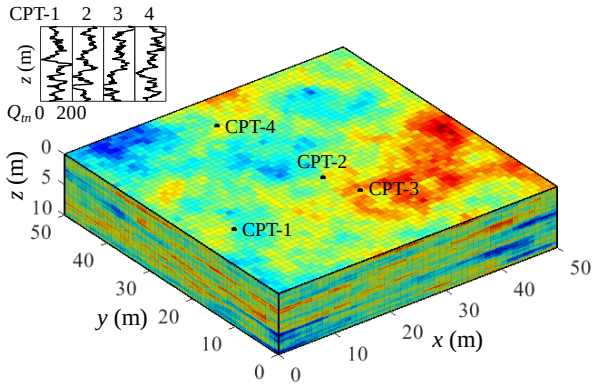

(a) Example I

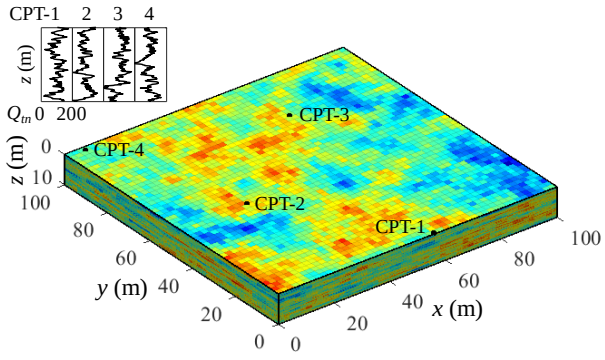

(b) Example II

Figure 2: Examples of virtual site and sampling plan.

n_h, as shown in Table 1. There is a total of 4^5 = 1024 scenarios in the virtual site analysis. In each scenario, 100 sampling plans, each of which contains n_h randomly distributed CPTs, are used to characterize the 3-D spatial variability of Q_{tn} using MLE.

Figure 2 presents two examples of virtual site with δ_v = 1 m and δ_h = 20 m. The corresponding sampling plans contain four CPTs performed at a same depth of 10 m, but in different sampling areas of 50×50 m^2 and 100×100 m^2, respectively. By applying MLE with the proposed matrix decomposition technique, the results of 3-D spatial variability characterization for the two examples are given in Table 2. Figure 3 illustrates

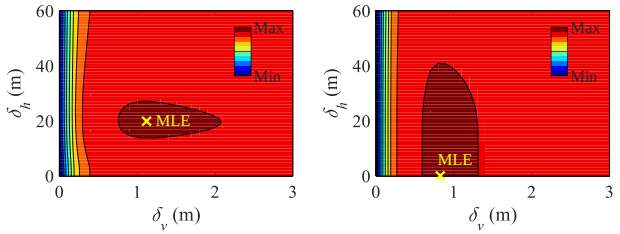

(a) Example I *(b) Example II*

Figure 3: Optimization of likelihood function in MLE.

the optimization of likelihood function in MLE. In Example I, the maximum likelihood estimates agree well with the corresponding true values and the COV values are relatively small for all parameters. This indicates that such a sampling plan can properly characterize the 3-D spatial variability and is effective to control the statistical uncertainty to a low level. In other words, it is possible to characterize the 3-D spatial variability with relatively limited data, as long as a proper characterization method and a proper sampling scheme are adopted. With respect to Example II, the estimates of (μ, σ, δ_v) are still reasonable, but the horizontal scale of fluctuation δ_h is unidentifiable, as shown in Figure 3(b). In this study, unidentifiable parameter refers to the parameter that is observationally equivalent (i.e., having the same likelihood) in a certain range. Particularly for δ_h, such a range usually covers zero and leads to a zero estimate of δ_h and an infinite COV. Unidentifiable sampling plan like Example II is what engineers should avoid in site investigation.

3.2. Design Criteria

To find out the reason why the two examples have opposite performances, the 3-D spatial variability are repeatedly quantified for all the 1024×100 sampling plans. Previous experience shows the largest statistical uncertainty mainly comes from δ_v and δ_h (Xiao et al., 2018). Therefore, this section adopts COV = $[\mathrm{COV}(\delta_v)^2+\mathrm{COV}(\delta_h)^2]^{1/2}$ as an integrated indicator of statistical uncertainty.

3.2.1. Distance criterion

As observed by Xiao et al. (2018), a small sounding distance facilitates the 3-D spatial variability characterization. It is rational because

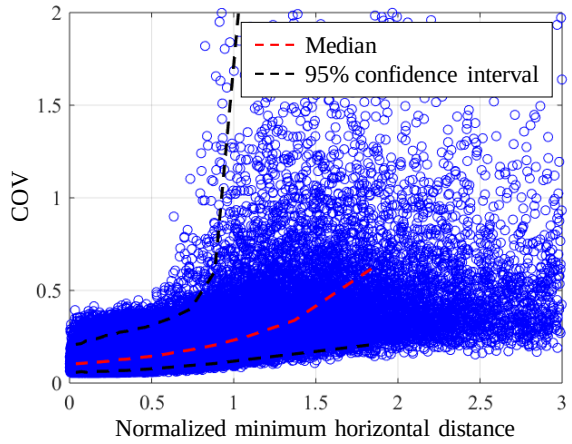

Figure 4: Effect of normalized minimum horizontal distance on statistical uncertainty.

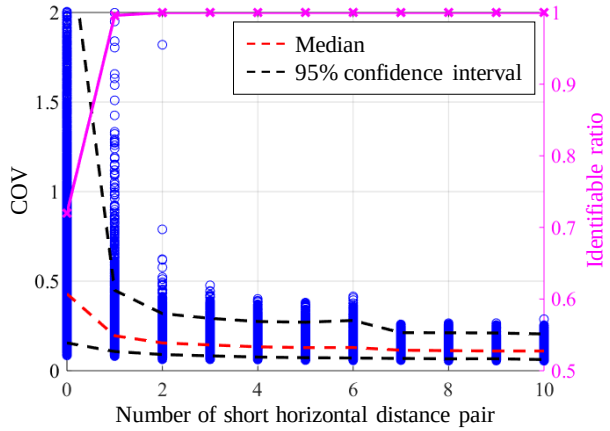

Figure 5: Effect of number of short horizontal distance pair on statistical uncertainty and identifiable ratio.

the spatial correlation for two locations in a large separation distance is almost negligible and unidentifiable.

To further validate this observation, all pairwise horizontal distances between every two CPTs in one sampling plan are calculated, and the minimum one is selected as a representative distance of the sampling plan and normalized by the corresponding true horizontal scale of fluctuation. For instance, the six pairwise horizontal distances in Example I are 19.4, 21.1, 29.7, 6.3, 21.2 and 27.5 m, respectively, and the normalized minimum horizontal distance $\Delta_{h,\min}$ is 0.32, between CPT-2 and CPT-3. Similarly, $\Delta_{h,\min}$ = 2.56 for Example II, also between CPT-2 and CPT-3.

Figure 4 plots the normalized minimum horizontal distances $\Delta_{h,\min}$ and the corresponding COV values for all sampling plans. For reference, the median line and the 95% confidence interval are also plotted in Figure 4 by red and black dashed lines, respectively. It is clear that the COV of estimated random field parameters is positively correlated with $\Delta_{h,\min}$ and there is an obvious turning point around $\Delta_{h,\min}$ = 1. When $\Delta_{h,\min} \leq 1$, the COV remains at a practically acceptable low level; and it significantly increases when $\Delta_{h,\min} > 1$. This is consistent with the observation in Xiao et al. (2018). The criterion that $\Delta_{h,\min} \leq 1$ is referred to as the distance criterion in this study. Since the actual horizontal scale of fluctuation is unknown in reality, it is suggested to carry out at least two closely located CPTs (e.g., 10 m) in practice.

In addition, Figure 5 presents the COV and the identifiable ratio against the number of short horizontal distance pair in one sampling plan. Herein, short horizontal distance pair refers to those distances less than the corresponding horizontal scale of fluctuation. The number is two and zero for Examples I and II, respectively. As shown in Figure 5, when the number is zero (i.e., $\Delta_{h,\min} > 1$), approximately 28% sampling plans confront the unidentifiable curse as Example II does. In contrast, almost all are identifiable for plans containing at least one short horizontal distance pair. Although such a ratio may vary considering different scenarios of virtual site and sampling scheme, the majority of unidentifiable sampling plans are certainly the ones with no short horizontal distance pair. Thus, it is undoubted that these plans are associated with a large statistical uncertainty, as shown in Figure 5.

On the other hand, Figure 5 also indicates that a great many short horizontal distance pairs would not help to reduce the COV significantly. More specifically, the median COV slightly decreases from 0.20 to 0.11, as the number of short horizontal distance pair increases from 1 to 10. In other words, for the investigated simplified scenarios, one short horizontal distance pair is sufficient to guarantee the identifiability and to

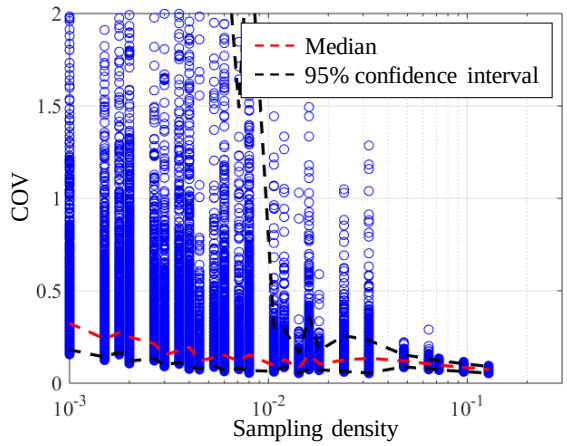

Figure 6: Effect of sampling density on statistical uncertainty.

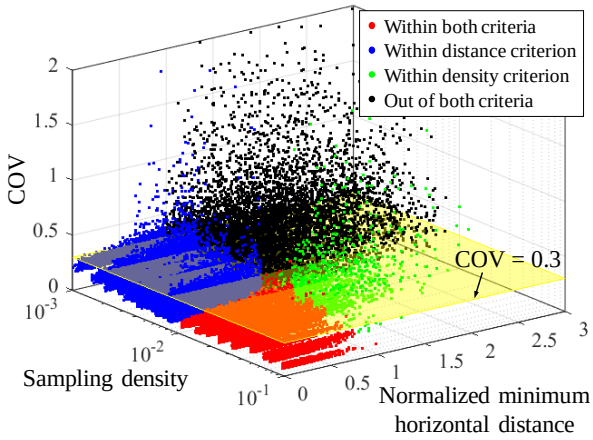

Figure 7: Region partition by two design criteria.

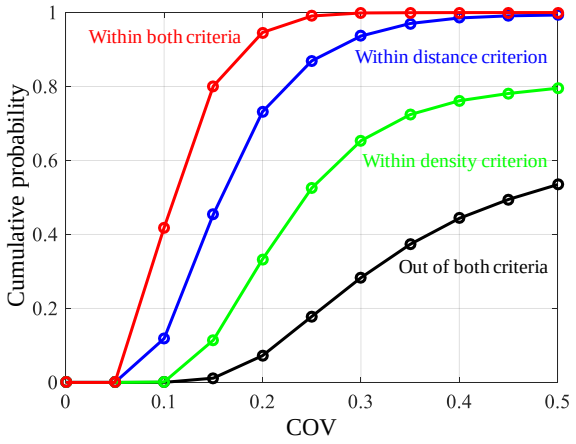

Figure 8: Cumulative probability of COV for different regions of sampling plan.

remain COV at a practically acceptable low level. There is no need to do many CPTs in a small region since a lot of information is redundant.

3.2.2. Density criterion

More intuitively, the simplest way that contributes to a smaller statistical uncertainty of 3-D spatial variability characterization is to increase the number or depth of CPT to collect more data records. The site investigation cost undoubtedly rises by this means. How to achieve the trade-off between the uncertainty reduction and cost is what engineers are concerned about.

For the purpose of comparison, define a sampling density as the product of sounding number n_h and sounding depth D over the sampling area A, i.e., $\varepsilon = n_h \times D/A$, in which the depth accounts for the impact of n_v. According to this definition, $\varepsilon = 0.016$ and 0.004 in Examples I and II, respectively.

Figure 6 demonstrates the effect of sampling density on the statistical uncertainty in 3-D spatial variability characterization. As expected, a higher sampling density results in a lower COV. Particularly when $\varepsilon \geq 0.01$, the 0.975 quantile of COV (i.e., the upper bound of 95% confidence interval) significantly falls to a practically acceptable low level. This means that the COV is highly likely to be small in such a case. The criterion that $\varepsilon \geq 0.01$ is referred to as the density criterion in this study.

With the increase in sounding number, the minimum horizontal distance either unchanges or decreases. Hence the two design criteria, namely the density criterion and the distance criterion, have a negative correlation to a certain degree. Figure 7 is the trivariate scatter diagram of Figure 4 and Figure 6. The space is divided into four regions by the two design criteria. As shown in Figure 7, the red region contains sampling plans satisfying both criteria; the blue and green regions contains those only within distance criterion and density criterion, respectively; and the black region contains those out of both criteria. Taking target COV = 0.3 as an example, the probabilities of COV $\leq$ 0.3 are equal to 99.9%, 93.6%, 65.3% and 28.3% for the red, blue, green and black regions, respectively. Likewise, the cumulative probability of COV for the four regions, as shown in Figure 8, can be obtained by setting different

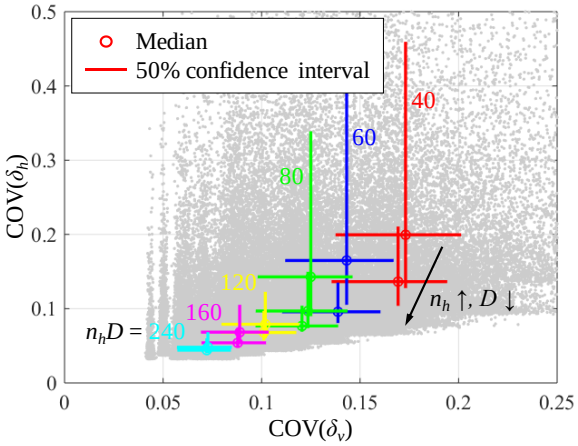

Figure 9: Effect of sounding number and depth on statistical uncertainty.

COV values. It is clear that the distance criterion is more effective than the density criterion to control the statistical uncertainty to a low level. By satisfying the two criteria simultaneously, the COV of 3-D spatial variability characterization can be well controlled to a low level (e.g., less than 0.3). Recall the two examples in the previous section. The sampling plan of Example I with $\Delta_{h,\min} = 0.32$ and $\varepsilon = 0.016$ is located at the red region, while the one of Example II with $\Delta_{h,\min} = 2.56$ and $\varepsilon = 0.004$ is located at the black region. It is not surprising that the first sampling plan performs much better than the second one.

Regarding the consistent sampling density, the impacts of sounding number n_h and sounding depth D may still be different. Figure 9 shows the scatters of COV(δ_v) and COV(δ_h) for all sampling plans. The sampling plans having the same values of n_hD are represented by their median and 50% confidence interval using the same color. For a given n_hD, a larger sounding number would bring about a slight decrease of COV(δ_v) as well as a significant decrease of COV(δ_h). This may be because a larger sounding number is more likely to have a shorter minimum horizontal distance, thus is easier to satisfy the distance criterion. Simply from the perspective of data utilization, a larger sounding number is more preferable than a deeper sounding depth, if the cost of drilling a new sounding is not considered. However, this only validates for sites with relatively homogenous soils. Some deeper CPT soundings are still required to facilitate the identification of complicated soil stratifications.

To sum up, for making a proper sampling scheme in spatial variability characterization, engineers can first determine a sounding number according to the density criterion, then conduct at least two closely located CPTs to fulfill the distance criterion. The remaining CPTs can be separated far to reduce the mapping uncertainty in the subsequent site mapping analysis (Li et al., 2016b). Such a sampling scheme is similar to so-called nested sampling proposed by DeGroot and Baecher (1993).

4. SUMMARY AND CONCLUSIONS

This paper proposes a matrix decomposition technique for MLE-based 3-D spatial variability characterization of soils. Results indicate that it is possible to characterize the 3-D spatial variability with relatively limited data, as long as a proper characterization method and a proper sampling scheme are adopted.

With the help of proposed approach, the sampling strategy to minimize the statistical uncertainty is explored. Through the virtual site analysis, two empirical design criteria are found, namely the distance criterion that the normalized minimum horizontal distances $\Delta_{h,\min} \leq 1$ and the density criterion that the sampling density $\varepsilon \geq 0.01$. The distance criterion is more effective than the density criterion. By satisfying the two criteria simultaneously, the statistical uncertainty of 3-D spatial variability characterization can be well controlled to a practically acceptable low level. Engineers can first determine a sounding number according to the density criterion, then conduct at least two closely located CPTs to fulfill the distance criterion.

In addition, it is also found that there is no need to do many CPTs in a small region, and a larger sounding number is better than a deeper sounding depth given the same total data amount. These observations are helpful to make a proper sampling scheme. More efforts on taking the uncertainties in model selection into the design of sampling strategy are still warranted.

5. ACKNOWLEGEMENTS

This work was supported by the National Key R&D Program of China (Project No. 2017YFC1501300), the National Natural Science Foundation of China (Project Nos. 51679174, and 51779189), and the Open Fund of Key Laboratory of Rock Mechanics in Hydraulic Structural Engineering, Ministry of Education of China (Project No. RMHSE1903). The financial support is gratefully acknowledged.

6. REFERENCES

Cao, Z., and Wang, Y. (2014). "Bayesian model comparison and selection of spatial correlation functions for soil parameters." *Structural Safety*, 49, 10–17.

Ching, J. Y., and Phoon, K. K. (2017). "Characterizing uncertain site-specific trend function by sparse Bayesian learning." *Journal of Engineering Mechanics*, 143(7), 04017028.

Ching, J., Wu, T. J., Stuedlein, A. W., and Bong, T. (2018). "Estimating horizontal scale of fluctuation with limited CPT soundings." *Geoscience Frontiers*, 9(6), 1597–1608.

DeGroot, D. J., and Baecher, G. B. (1993). "Estimating autocovariance of in-situ soil properties." *Journal of Geotechnical Engineering*, 119(1), 147–166.

Fenton, G. A. (1999). "Estimation for stochastic soil models." *Journal of Geotechnical and Geoenvironmental Engineering*, 125(6), 470–485.

Fenton, G. A., and Griffiths, D. V. (2005). "Three-dimensional probabilistic foundation settlement." *Journal of Geotechnical and Geoenvironmental Engineering*, 131(2), 232–239.

Li, D. Q., Xiao, T., Cao, Z. J., Zhou, C. B., and Zhang, L. M. (2016a). "Enhancement of random finite element method in reliability analysis and risk assessment of soil slopes using Subset Simulation." *Landslides*, 13(2), 293–303.

Li, Y. J., Hicks, M. A., and Vardon, P. J. (2016b). "Uncertainty reduction and sampling efficiency in slope designs using 3D conditional random fields." *Computers and Geotechnics*, 79, 159–172.

Liu, W. F., and Leung, Y. F. (2018). "Characterising three-dimensional anisotropic spatial correlation of soil properties through in situ test results." *Géotechnique*, 68(9), 805–819.

Papaioannou, I., and Straub, D. (2017). "Learning soil parameters and updating geotechnical reliability estimates under spatial variability–theory and application to shallow foundations." *Georisk: Assessment and Management of Risk for Engineered Systems and Geohazards*, 11(1), 116–128.

Vanmarcke, E. H. (2010). *Random fields: analysis and synthesis (revised and expanded new edition)*. Singapore: World Scientific Publishing Co. Pte. Ltd.

Wang, Y., Au, S. K., and Cao, Z. (2010). "Bayesian approach for probabilistic characterization of sand friction angles." *Engineering Geology*, 114(3), 354–363.

Xiao, T., Li, D. Q., Cao, Z. J., Au, S. K., and Phoon, K. K. (2016). "Three-dimensional slope reliability and risk assessment using auxiliary random finite element method." *Computers and Geotechnics*, 79, 146–158.

Xiao, T., Li, D. Q., Cao, Z. J., and Tang, X. S. (2017). "Full probabilistic design of slopes in spatially variable soils using simplified reliability analysis method." *Georisk: Assessment and Management of Risk for Engineered Systems and Geohazards*, 11(1), 146–159.

Xiao, T., Li, D. Q., Cao, Z. J., and Zhang, L. M. (2018). "CPT-based probabilistic characterization of three-dimensional spatial variability using MLE." *Journal of Geotechnical and Geoenvironmental Engineering*, 144(5), 04018023.

Yoshida, I., Tasaki, Y., Otake, Y., and Wu, S. (2018). "Optimal sampling placement in a Gaussian random field based on value of information." *ASCE-ASME Journal of Risk and Uncertainty in Engineering Systems, Part A: Civil Engineering*, 4(3), 04018018.